Electronic topological transition in zinc under pressure: An x-ray absorption spectroscopy study

G. Aquilanti,[1,*] A. Trapananti,[1] M. Minicucci,[2] F. Liscio,[3] A. Twaróg,[4] E. Principi,[2] and S. Pascarelli[1]
[1]*European Synchrotron Radiation Facility, 6 rue Jules Horowitz, Boîte Postale 220, 38043 Grenoble Cedex, France*
[2]*CNISM, CNR-INFM, Dipartimento di Fisica, Università degli Studi di Camerino, via Madonna delle Carceri 9, 62032 Camerino (Macerata), Italy*
[3]*Laboratoire de Thermodynamique et Physico-Chimie Métallurgiques, ENSEEG, Boîte Postale 75, 38402 Saint Martin d'Hères, France*
[4]*Faculty of Physics, Warsaw University of Technology, Koszykowa 75, 00-662 Warsaw, Poland*
(Received 10 January 2007; revised manuscript received 18 May 2007; published 3 October 2007)

Zinc metal has been studied at high pressure using x-ray absorption spectroscopy. In order to investigate the role of the different degrees of hydrostaticity on the occurrence of structural anomalies following the electronic topological transition, two pressure transmitting media have been used. Results show that the electronic topological transition, if it exists, does not induce an anomaly in the local environment of compressed Zn as a function of hydrostatic pressure and any anomaly must be related to a loss of hydrostaticity of the pressure transmitting medium. The near-edge structures of the spectra, sensitive to variations in the electronic density of states above the Fermi level, do not show any evidence of electronic transition whatever pressure transmitting medium is used.

DOI: 10.1103/PhysRevB.76.144102 PACS number(s): 61.10.Ht, 61.50.Ks, 64.70.Kb

I. INTRODUCTION

Zinc and its isoelectronic counterpart, cadmium, are unique among divalent hexagonal closed packed (hcp) structured metals. For Zn, the c/a axial ratio is equal to 1.856 (Ref. 1) (1.886 for Cd) and exceeds by about 14% the ideal value $[\sqrt{(8/3)}]$ of hcp structures. As a consequence, the structure of Zn is quite distorted and the local environment is not given by 12 first neighbors like in a regular hcp metal, but by 6 first neighbors at 2.664 Å and 6 second neighbors at 2.91 Å. The effect of the large axial ratio c/a in Zn is also exhibited in its Fermi surface topology and, accordingly, many of its solid state properties are highly anisotropic. The fact that the Fermi surface of Zn differs from that of normal hcp metals gives rise to a giant Kohn anomaly in the zone center,[2] i.e., in the long wavelength phonons region. Such anomaly can substantially affect low-energy acoustic phonons producing abrupt changes of phonon frequencies at wave vectors that are related to extremal dimensions of the Fermi surface.[3] Theoretical studies have been debating these phenomena in terms of density of states at the Fermi energy $N(E_F)$ and, in particular, in terms of the asymmetric charge distribution of the p states that mainly contribute to the $N(E_F)$.[4]

Upon compression, the axial ratio c/a decreases toward the ideal value because of an important anisotropy of the linear compressibility. As the ratio c/a diminishes, qualitative changes in the band structure occur. Following a compression, the electronic band extremum may shift through the Fermi level E_F. In this case, new elements appear on the Fermi surface that change its topology. Such topology change, referred as electronic topological transition (ETT), can lead to anomalies in transport, thermodynamic, and vibrational properties, as well as in the lattice structure. In this context, the high pressure behavior of Zn is of particular interest.

Many experimental works dealing with structural studies of Zn under pressure aimed to detect an anomaly in the trend of the c/a axial ratio under pressure. Such anomaly was first reported by Lynch and Drickamer[5] around 7 GPa, although this result was not confirmed later by McWham[6] and by Schulte *et al.*[7] More recently, Takemura *et al.* performed several angle dispersive x-ray diffraction studies[8–11] using different pressure transmitting media (PTM) obtaining different results. They showed that the occurrence of an anomaly of c/a as a function of pressure could be related to the nonhydrostaticity of the PTM. Contradictory results can also be found among the studies aimed to detect an anomaly in the lattice dynamics following the ETT. An anomalous high pressure behavior of the acoustic phonon frequencies is supported by both Mössbauer studies[12–14] and an inelastic neutron scattering (INS) study,[15] though the two results are in contrast as a phonon softening and hardening were found by the Mössbauer and INS studies, respectively. On the other hand, Klotz *et al.*[16] did not report any anomaly in a following INS work. In an intermediate position is a Raman study[17] where an anomaly has been observed in the pressure dependence of the linewidth around 10 GPa, but not in the frequency of the Raman mode.

The conflicting experimental results have prompted several subsequent theoretical investigations on the structure and electronic properties of Zn at high pressure.[3,18–22] Band structure and density of states calculations are made to predict the occurrence of the ETT in Zn. Total energy calculations are made in order to determine the crystallographic axes at different volumes by finding the minimum in the total energy evidencing possible anomalies in the c/a axial ratio.

A large consensus exists between the theoretical studies about the occurrence of, at least, one ETT in Zn under pressure, though different works and methods calculated and found one or more ETTs in different points of the Brillouin zone. However, contradictory results concern the question whether or not such ETT(s) are accompanied and/or coupled with the anomaly in c/a. Meenakshi *et al.*,[18] Novikov *et al.*,[3] Godwal *et al.*,[22] Kechin,[21] and Li and Tse[23] supported the occurrence of the anomaly in c/a. Li and Tse also found a

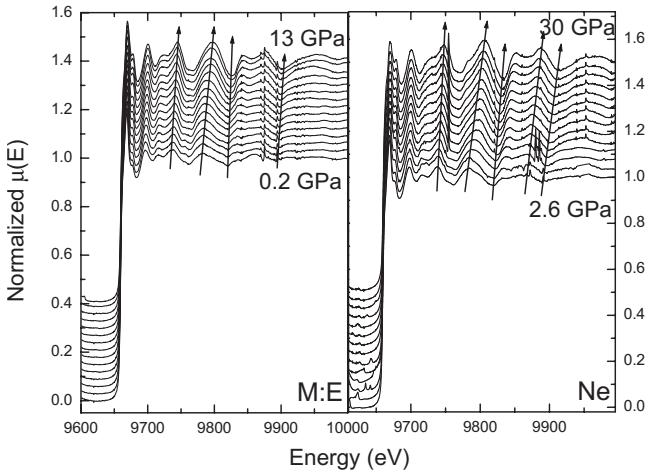

FIG. 1. Normalized XAS spectra using a mixture of 4:1 methanol:ethanol (M:E) (left panel) and Ne (right panel) as pressure transmitting medium. The arrows highlight the evolution with pressure of the main features (maxima and minima) of the modulations of the absorption cross section.

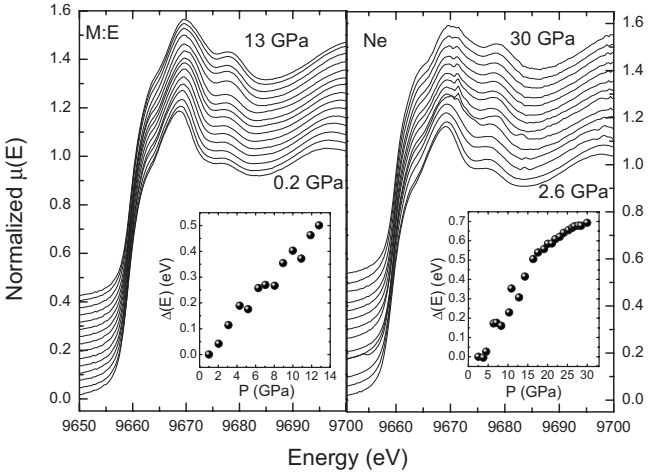

FIG. 2. XANES spectra using M:E (left panel) and Ne (right panel) as PTM. The insets show the energy variation of the maximum of the derivative of the absorption as a function of pressure.

softening of acoustic modes near the Γ point at the pressure where the c/a ratio shows a discontinuity. In contrast, Steinle-Neumann *et al.*[20] showed that the ETT is independent of the calculated anomaly in the a axis compressibility and, in particular, that the trend of the a axis strongly depends on the number of the k sampling of the calculations. This overview shows that the high pressure behavior of Zn is an example not only of controversy but also of extensive interplay between theory and experiment.

No x-ray absorption spectroscopy (XAS) study of Zn under pressure exists in literature. X-ray absorption fine structure (XAFS) refers to the oscillatory structure in the x-ray absorption coefficient above an x-ray absorption edge. This is a unique signature of a given material and depends on its atomic structure and vibrational properties.[24] The aim of this study is twofold: (i) to give a direct evidence for the ETT in solid Zn under pressure by probing the pressure-induced changes in the electronic density of states above the Fermi level through the variation of the x-ray absorption near-edge structure (XANES) and (ii) to detect a possible anomalous dependence with pressure of the nearest neighbor distances connected to a change of the Fermi surface topology.

The paper is organized as follows: In Sec. II, we report the experimental details of the XAFS measurements. In Sec. III, we present the data and their evolution from a qualitative point of view. The details of the data analysis together with the results are presented in Sec. IV. In Sec. V, we discuss the results, and in Sec. VI, we give several conclusions.

II. EXPERIMENTAL DETAILS

The XAS data have been recorded at the dispersive XAS beamline of ESRF, ID24 (Ref. 25) at the Zn K edge (9659 eV).

The sample consisted of a foil of 10 μm thickness from Goodfellow (purity of 99.9%). A preliminary angle dispersive x-ray diffraction pattern recorded on BM08 using a monochromatic beam of $\lambda=0.355$ Å and an image plate as detector showed a random orientation of the crystallites in the foil.

The pressure was generated by a Le Toullec diamond anvil cell (DAC) and was measured before and after each XAS spectrum using the ruby fluorescence method.[26] The ruby sphere was placed close to the border of the cell volume, while the sample was placed at the center. This is necessary for XAS experiments to avoid any interaction between the x-ray beam and the ruby, detrimental to the data quality. The possible nonhydrostaticity leads to a pressure gradient in the sample volume. In particular, the pressure is higher at the center of the cell volume (where the sample for XAS measurements is placed) and decreases toward the border of the cell volume (where the ruby sphere is placed). Therefore, in the present experiments, the ruby fluorescence gives a measure of the pressure that is less than the pressure to which the sample for XAS measurements is actually subjected. Two experiments were performed: the first up to 13 GPa using a 4:1 mixture of methanol:ethanol (M:E) as PTM, and the second up to 30 GPa using neon. The M:E is supposed to yield quasihydrostatic conditions up to 10 GPa.[27–30] Previous experiments[31] suggest that the strength of solid Ne above 100 GPa is sufficiently low that the material can be used as a quasihydrostatic medium over this pressure range.

A reference spectrum of Zn foil at ambient conditions was recorded per each spectrum as a function of pressure. Such a procedure is necessary whenever small changes of the absorption edge energy might be detected at a phase transition. Bragg reflections of the diamond anvils limited the exploitable k range of the data to a maximum of about 9 Å^{-1}. Other less intense Bragg reflections were present at lower k (see Figs. 1–3) without being detrimental for the data analysis.

III. QUALITATIVE DESCRIPTION OF DATA AND EVOLUTION WITH PRESSURE

In Fig. 1, we present the data recorded during the two experiments normalized to the jump at the absorption edge at

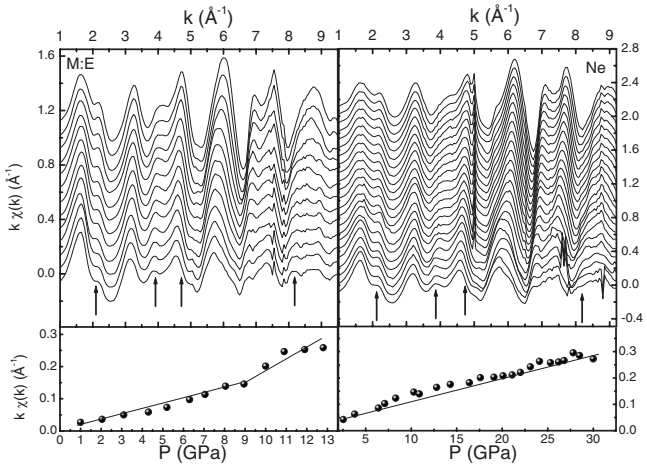

FIG. 3. Extracted $k\chi(k)$ signals (vertically shifted by 0.1 Å^{-1}) using M:E (top-left panel) and Ne (top-right panel). Intensity of $k\chi(k)$ signals as a function of pressure at k=4.75 Å^{-1} for the M:E data set (bottom-left panel) and for the Ne data set (bottom-right panel).

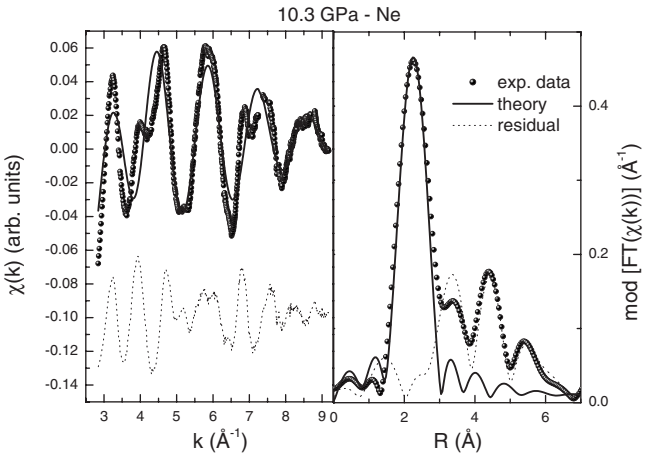

FIG. 4. Left panel: Comparison between the experimental EXAFS spectrum at 10.3 GPa (dots) using Ne as PTM and the best-fit calculation (solid curve) corresponding to a single-distance shell of six Zn atoms. The bottom curve represents the residual function. Right panel: Comparison between the modulus of the Fourier transform of the experimental EXAFS spectrum at 10.3 GPa (dots) using Ne as PTM and the modulus of the Fourier transform of the best-fit calculation (solid curve) corresponding to a single-distance shell of six Zn atoms. The residual curve is the dotted curve.

selected pressures. The data do not show any dramatic change up to the maximum pressure. The arrows highlight the evolution with pressure of the main features (maxima and minima) of the modulations of the absorption cross section. As pressure increases (bottom to top), the main frequency of the oscillations decreases as a consequence of bond length contraction. According to the electric dipole selection rules, the XANES spectra directly probe the density of unoccupied states with p symmetry. Therefore, the variations as a function of pressure of the near-edge structures of the spectra are a probe for pressure-induced changes in the electronic density of states above the Fermi level and may be a direct evidence of the ETT.

The near-edge part of the spectra for the two experiments is shown in Fig. 2. Although the data show a decrease of the intensity of the white line with respect to the first oscillation at about 9680 eV, such modifications are gradual as a function of pressure and no discontinuity can be observed. The two insets of Fig. 2 show the energy evolution with pressure of the maximum of the derivative of the absorption spectra with respect to the first point recorded in the two experiments at 1 and 2.55 GPa, respectively. Even in this case, the evolution toward high energies of the onset of the absorption is continuous for both experiments.

The experimental XAFS $\chi(k)$ was obtained after subtracting the embedded-atom absorption background from the measured absorption coefficient[32] and normalizing by the edge step. The curves for the two experiments, multiplied by k, are shown in Fig. 3 (top panels).

The evolution of the extracted signals is continuous with pressure. At specific k values, indicated by arrows on the top panels of Fig. 3, the differences between the signals at low and high pressures are more evident. To highlight such changes, we plotted the intensity of the $k\chi(k)$ signals as a function of pressure at these values of k. The bottom panels of Fig. 3 report, as an example, the trend of the $k\chi(k)$ as a function of pressure for k=4.75 Å^{-1}. The continuous line is a guide for the eyes. There is no discontinuity for the Ne data set, while a small one can be observed at 9 GPa for the M:E data set. Similar results were obtained at different k values.

IV. EXTENDED X-RAY ABSORPTION FINE STRUCTURE DATA ANALYSIS AND RESULTS

The EXAFS data analysis was carried out using the GNXAS package.[33] The main contribution to the total EXAFS signal is given by the single scattering between the photoabsorber and the first six neighbors. Given the k range of the EXAFS data, limited by the Bragg reflections arising from the diamond anvils, we analyzed the data using a single-distance shell to limit the number of free parameters. A symmetric distribution of bond distances was used, characterized by the following structural parameters: R (average bond distance) and σ^2 (relative mean square displacement or EXAFS Debye-Waller factor). The best-fit calculation compared with the experimental EXAFS spectrum for the data at 10.3 GPa using Ne as PTM is shown in the left panel of Fig. 4.

The residual function (bottom curve) contains frequencies associated with higher distance shells and multiple scattering contributions. However, the first peak of the Fourier transform of the experimental data is well reproduced by the best-fit calculation, showing that the structural parameters relative to the first neighbors are correctly determined within the reported errors.

Figure 5 reports the first neighbor average distances and EXAFS Debye-Waller factors (left and right panels, respectively) obtained from the experimental data collected using M:E as PTM. First neighbor distances R calculated from the lattice parameters reported by Takemura[10] (solid line) are

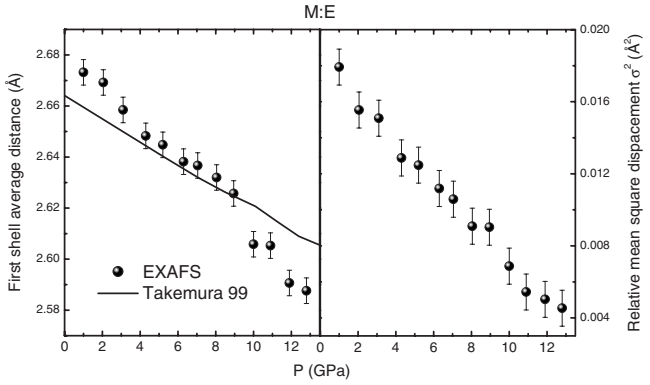

FIG. 5. First shell distance R and EXAFS Debye-Waller factor σ^2 (left and right panels, respectively) as a function of pressure for Zn obtained from XAFS analysis for the data recorded using M:E as PTM. The distances R are compared with those obtained by Takemura (Ref. 10) (continuous line).

compared with XAFS experimental results. The EXAFS results are in good agreement with Takemura's up to $P=10$ GPa. After this pressure, an evident discrepancy can be observed: in particular, the XAFS results show an increase of bond compressibility after 10 GPa. The present result appears to be counterintuitive and it will be discussed in the next section. The evolution as a function of pressure of the EXAFS Debye-Waller factor does not show any discontinuity within the error up to the maximum pressure reached.

Figure 6 reports the first neighbor average distances and EXAFS Debye-Waller factors (left and right panels, respectively) of the experiment performed using neon as PTM. First neighbor distances R calculated from the lattice parameters reported by Takemura[10] are compared with XAFS experimental results. The EXAFS results are in good agreement with Takemura's up to the maximum pressure reached. The first neighbor average distance decreases smoothly as a function of pressure with no discontinuity whatsoever. The

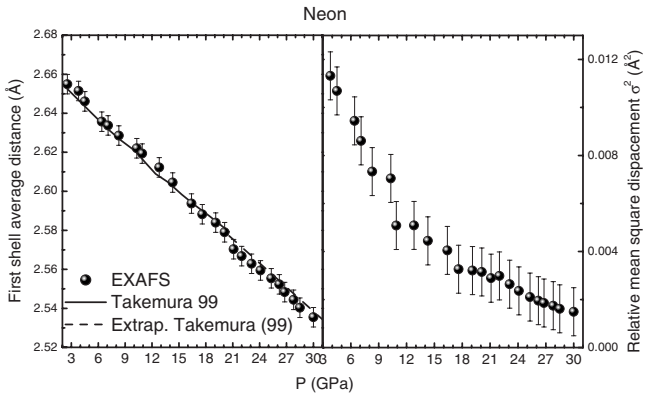

FIG. 6. First shell distance R and EXAFS Debye-Waller factor σ^2 (left and right panels, respectively) as a function of pressure for Zn obtained from XAFS analysis for the data recorded using Ne as PTM. The distances R are compared with those obtained by Takemura (Ref. 10) (continuous line). The dotted line represents an extrapolation of R in the pressure range not covered by Takemura (Ref. 10).

EXAFS Debye-Waller factor does not show any discontinuity within the error up to the maximum pressure reached. Nonetheless, it does not decrease linearly with increasing P as the first neighbor distance does. This must be attributed to an overestimation at low pressures ($P \leqslant 8$ GPa) due to the used fitting procedure. At ambient pressure, the first and the second shell of neighbors are at distances with respect to the photoabsorber atom such that the corresponding calculated single scattering signals are in antiphase in the k range of interest ($k=3-9$ Å^{-1}). Under compression, the phases of the two calculated signals approach each other, but they never become equal. That is to say, although upon compression Zn approaches the ideal hcp structured metals, it never possesses (at least up to 30 GPa) a local environment given by 12 nearest neighbors. At low pressures, the experimental signal is anomalously dumped by the fact that the two main contributions (first and second shell neighbor single scattering signals) are in antiphase. This effect, on one side, prevents the accurate determination of the second shell neighbor distance and, on the other side, yields to an overestimation of the variance (σ^2) of the first shell distance distribution functions.

V. DISCUSSION

We found that the evolution of the first neighbor average distance R as a function of pressure depends on the PTM used. In particular, the first neighbor average distance R presents a discontinuity at about 10 GPa when M:E is used as PTM. This is in agreement with Takemura[9] according to which an anomaly on the structure of Zn under pressure must be attributed to a loss of hydrostaticity of the PTM. Our result can be explained in terms of pressure gradient inside the sample volume of the DAC in case of nonhydrostatic conditions. The fact that the ruby sphere for the pressure measurements was placed close to the border of the cell volume together with a pressure gradient that is associated with nonhydrostatic conditions led to an underestimation of the pressure relative to the EXAFS spectra measured on a sample placed at the center of the cell volume. The EXAFS spectra recorded using M:E as PTM at reported pressures beyond 10 GPa are, in fact, relative to higher pressure conditions on the sample. Therefore, we do not attribute the discontinuity of R, as reported in the left panel of Fig. 5, to an anomaly following an ETT in compressed Zn nor to an effect due to strain on the sample subjected to nonhydrostatic conditions. This last hypothesis is ruled out as EXAFS is less sensitive to nonhydrostaticity and uniaxial strain, since it measures average bond distances directly. We attribute the above discussed discontinuity of R to an effect of pressure gradient that, if taken into account, would eliminate or at least decrease such discontinuity. This argumentation is supported by the results obtained using Ne as PTM. In this case, since the pressure gradients were negligible as the quasihydrostaticity was conserved up to the maximum pressure reached, no discontinuity was observed.

EXAFS probes an average of configurations around the photoabsorber and the bond distances are spread in a distribution $g(r)$. The width of such a distribution is taken into account by the mean square relative displacement σ^2

(EXAFS Debye-Waller factor: $e^{-2\sigma^2 k^2}$). The Debye-Waller factor contains two contributions: a thermal and a structural contribution linked to the local vibrational dynamics and to the local structural distortions, respectively. Such parameter as obtained by the EXAFS data analysis does present a smooth trend and no anomalies as a function of pressure in both experiments. However, it is worth to discuss how the EXAFS Debye-Waller factor could be a useful signature of the occurrence of an ETT in Zn.

If we consider the thermal part only of the EXAFS Debye-Waller factor, in the case of a monatomic Bravais crystal and assuming the validity of the harmonic approximation, it can be linked to the frequency of the vibrational mode as follows:[34]

$$\sigma_i^2 = \frac{\hbar}{2\mu} \int \frac{d\omega}{\omega} \rho_i(\omega) \coth\left(\frac{\beta\hbar\omega}{2}\right),$$

where μ is the reduced mass of the photoabsorber M_0 and the neighbor M_i, $\beta = 1/k_B T$, and $\rho_i(\omega)$ is a projected density of modes which properly weights the contribution of each mode to relative vibrational motion along the bond direction. Only the short wavelength modes are relevant to the vibration of the first neighbor atoms. However, the possible destruction of the giant Kohn anomaly following the occurrence of the ETT would concern an anomaly in the long wavelength phonon modes that, for what discussed before, unlikely could be detected by an anomaly of the EXAFS Debye-Waller factor. Concerning the structural contribution of the EXAFS Debye-Waller factor, a theoretical prediction exists[3] according to which at the occurrence of the ETT several values of c/a might coexist, keeping the energy almost constant. This would induce in the local structure an increase of disorder that would be possibly detected by an anomalous increase in the trend as a function of pressure of the Debye-Waller factor. This effect, if it existed, would compete with a normal decrease of the EXAFS Debye-Waller factor as an effect of the bond distance reduction due to compression.

VI. CONCLUSIONS

In conclusion, we performed two EXAFS experiments on Zn under pressure using different PTM of different hydrostaticity: M:E and Ne. The XANES part of the spectra shows a continuous evolution without any anomaly and/or discontinuity for both data sets. The EXAFS signals show for both data sets an increase of the intensity of the oscillations. For the M:E set, the signals show a discontinuity for several k values at about 10 GPa, while for the Ne set, a continuous evolution is shown up to the maximum pressure. The quantitative EXAFS analysis shows for the M:E data set a discontinuity in the trend of R at $\sim$10 GPa and a smooth variation of EXAFS Debye-Waller factor and for the Ne a smooth variation of R and σ^2. Therefore, the ETT, if it exists, does not induce an anomaly in the local environment of compressed Zn as a function of *quasihydrostatic* pressure. Any anomaly *must* be related to a loss of hydrostaticity of the PTM. The XANES features, sensitive to changes in the electronic density of states, do not show evidence of electronic transition whatever pressure transmitting medium is used.

ACKNOWLEDGMENTS

We acknowledge the European Synchrotron Radiation Facility for provision of in-house research beamtime. We are also grateful to M. Merlini for sample characterization on beamline BM08 (ESRF) and to C. Meneghini for useful discussion.

*aquilanti@esrf.fr

[1] J. Donohue, *The Structures of the Elements* (Wiley, New York, 1974), pp. 225–230.
[2] W. Kohn, Phys. Rev. Lett. **2**, 393 (1959).
[3] D. L. Novikov, A. J. Freeman, N. E. Christensen, A. Svane, and C. O. Rodriguez, Phys. Rev. B **56**, 7206 (1997).
[4] E. Bodenstedt, B. Perscheid, and S. Nagel, Z. Phys. B: Condens. Matter **63**, 9 (1986).
[5] R. W. Lynch and H. G. Drickamer, J. Phys. Chem. Solids **26**, 63 (1965).
[6] D. B. McWhan, J. Appl. Phys. **36**, 664 (1965).
[7] O. Schulte, A. Nikolaenko, and W. B. Holzapfel, High Press. Res. **6**, 169 (1991).
[8] K. Takemura, Phys. Rev. Lett. **75**, 1807 (1995).
[9] K. Takemura, Phys. Rev. B **56**, 5170 (1997).
[10] K. Takemura, Phys. Rev. B **60**, 6171 (1999).
[11] K. Takemura, Y. Hiroshi, F. Hiroshi, and K. Takumi, Phys. Rev. B **65**, 132107 (2002).
[12] W. Potzel, W. Adlassnig, J. Moser, C. Schäfer, M. Steiner, and G. M. Kalvius, Phys. Rev. B **39**, 8236 (1989).
[13] W. Potzel, M. Steiner, H. Karzel, W. Schiessl, M. Köfferlein, G. M. Kalvius, and P. Blaha, Phys. Rev. Lett. **74**, 1139 (1995).
[14] M. Steiner, W. Potzel, H. Karzel, W. Schiessl, M. Köfferlein, G. M. Kalvius, and P. Blaha, J. Phys.: Condens. Matter **8**, 3581 (1996).
[15] J. G. Morgan, R. B. Von Dreele, P. Wochner, and S. M. Shapiro, Phys. Rev. B **54**, 812 (1996).
[16] S. Klotz, M. Braden, and J. M. Besson, Phys. Rev. Lett. **81**, 1239 (1998).
[17] H. Olijnyk, A. P. Jephcoat, D. L. Novikov, and N. E. Christensen, Phys. Rev. B **62**, 5508 (2000).
[18] S. Meenakshi, V. Vijayakumar, B. K. Godwal, and S. K. Sikka, Phys. Rev. B **46**, 14359 (1992).
[19] D. L. Novikov, M. I. Katsnelson, A. V. Trefilov, A. J. Freeman, N. E. Christensen, A. Svane, and C. O. Rodriguez, Phys. Rev. B **59**, 4557 (1999).
[20] G. Steinle-Neumann, L. Stixrude, and R. E. Cohen, Phys. Rev. B **63**, 054103 (2001).
[21] V. V. Kechin, Phys. Rev. B **63**, 045119 (2001).
[22] B. K. Godwal, P. Modak, and R. S. Rao, Solid State Commun. **125**, 401 (2003).
[23] Z. Li and J. S. Tse, Phys. Rev. Lett. **85**, 5130 (2000).

[24] P. A. Lee, P. H. Citrin, P. Eisenberger, and B. M. Kinkaid, Rev. Mod. Phys. **53**, 769 (1981).
[25] S. Pascarelli, O. Mathon, and G. Aquilanti, J. Alloys Compd. **362**, 33 (2004).
[26] R. A. Forman, G. J. Piermarini, J. D. Barnett, and S. Block, Science **176**, 284 (1972).
[27] G. J. Piermarini, S. Block, and J. D. Barnett, J. Appl. Phys. **44**, 5377 (1973).
[28] J. H. Eggert, L. W. Xu, R. Z. Che, L. C. Chen, and J. F. Wang, J. Appl. Phys. **72**, 2453 (1992).
[29] B. Grocholski and R. Jeanloz, J. Chem. Phys. **123**, 204503 (2005).
[30] R. J. Angel, M. Bujak, J. Zhao, G. D. Gatta, and S. D. Jacobsen, J. Appl. Crystallogr. **40**, 26 (2007).
[31] R. J. Hemley, C. S. Zha, A. P. Jephcoat, H. K. Mao, L. W. Finger, and D. E. Cox, Phys. Rev. B **39**, 11820 (1989).
[32] M. Newville, P. Līviņš, Y. Yacoby, J. J. Rehr, and E. A. Stern, Phys. Rev. B **47**, 14126 (1993).
[33] A. Filipponi, A. Di Cicco, and C. R. Natoli, Phys. Rev. B **52**, 15122 (1995).
[34] E. Sevillano, H. Meuth, and J. J. Rehr, Phys. Rev. B **20**, 4908 (1979).